

Inter-comparison of low-cost sensors for measuring the mass concentration of occupational aerosols

Sinan Sousan, Kirsten Koehler, Geb Thomas, Jae Hong Park, Michael Hillman, Andrew Halterman & Thomas M. Peters

To cite this article: Sinan Sousan, Kirsten Koehler, Geb Thomas, Jae Hong Park, Michael Hillman, Andrew Halterman & Thomas M. Peters (2016) Inter-comparison of low-cost sensors for measuring the mass concentration of occupational aerosols, *Aerosol Science and Technology*, 50:5, 462-473, DOI: [10.1080/02786826.2016.1162901](https://doi.org/10.1080/02786826.2016.1162901)

To link to this article: <http://dx.doi.org/10.1080/02786826.2016.1162901>



[View supplementary material](#)



Accepted author version posted online: 10 Mar 2016.

Published online: 10 Mar 2016.



[Submit your article to this journal](#)



Article views: 795



[View related articles](#)



[View Crossmark data](#)



Citing articles: 16 [View citing articles](#)

Inter-comparison of low-cost sensors for measuring the mass concentration of occupational aerosols

Sinan Sousan^a, Kirsten Koehler^b, Geb Thomas^c, Jae Hong Park^a, Michael Hillman^c, Andrew Halterman^d, and Thomas M. Peters^a

^aDepartment of Occupational and Environmental Health, University of Iowa, Iowa City, Iowa, USA; ^bEnvironmental Health Sciences, Johns Hopkins Bloomberg School of Public Health, Baltimore, Maryland, USA; ^cDepartment of Mechanical and Industrial Engineering, University of Iowa, Iowa City, Iowa, USA; ^dDepartment of Chemical and Biochemical Engineering, University of Iowa, Iowa City, Iowa, USA

ABSTRACT

Low-cost sensors are effective for measuring the mass concentration of ambient aerosols and second-hand smoke in homes, but their use at concentrations relevant to occupational settings has not been demonstrated. We measured the concentrations of four aerosols (salt, Arizona road dust, welding fume, and diesel exhaust) with three types of low-cost sensors (a DC1700 from Dylos and two commodity sensors from Sharp), an aerosol photometer, and reference instruments at concentrations up to $6500 \mu\text{g}/\text{m}^3$. Raw output was used to assess sensor precision and develop equations to compute mass concentrations. EPA and NIOSH protocols were used to assess the mass concentrations estimated with low-cost sensors compared to reference instruments. The detection efficiency of the DC1700 ranged from 0.04% at $0.1 \mu\text{m}$ to 108% at $5 \mu\text{m}$, as expected, although misclassification of fine and coarse particles was observed. The raw output of the DC1700 had higher precision (lower coefficient of variation, $CV = 7.4\%$) than that of the two sharp devices ($CV = 25\%$ and 17%), a finding attributed to differences in manufacturer calibration. Aerosol type strongly influenced sensor response, indicating the need for on-site calibration to convert sensor output to mass concentration. Once calibrated, however, the mass concentration estimated with low-cost sensors was highly correlated with that of reference instruments ($R^2 = 0.99$). These results suggest that the DC1700 and Sharp sensors are useful in estimating aerosol mass concentration for aerosols at concentrations relevant to the workplace.

ARTICLE HISTORY

Received 5 November 2015
Accepted 21 January 2016

EDITOR

Tiina Reponen

Introduction

Environmental and occupational exposures to fine particulate matter (particles smaller than $2.5 \mu\text{m}$) and coarse particulate matter (particles between $2.5 \mu\text{m}$ and $10 \mu\text{m}$) have been associated with adverse health effects and increased mortality rates (Dockery et al. 1993; Grant 2009). Such exposures include dust, sea salt, automobile exhaust, industrial emissions, welding fumes, sawdust, animal waste, and crop dust (Seinfeld and Pandis 2012). Exposure to specific aerosols leads to specific adverse health outcomes: coal mine dust to adverse respiratory changes (Henneberger and Attfield 1997); welding fume to respiratory diseases and lung cancer (Antonini 2003); and diesel fume to pulmonary disease (Hart et al. 2012) and lung cancer (Lipsett and Campleman 1999).

The United States government uses mass-based regulations to protect the public and workers from harmful exposure from inhalation of harmful particles. The

National Ambient Air Quality Standards (NAAQS) under the authority of the Environmental Protection Agency (EPA) specify that states maintain the mass concentration of ambient particles smaller than $2.5 \mu\text{m}$ ($\text{PM}_{2.5}$) below $35 \mu\text{g}/\text{m}^3$ daily and $15 \mu\text{g}/\text{m}^3$ annually, and the mass concentration of particles smaller than $10 \mu\text{m}$ (PM_{10}) below $150 \mu\text{g}/\text{m}^3$ daily (EPA 2013). In the workplace, employers must demonstrate that the personal exposures of workers do not exceed occupational exposure limits set by the Occupational Safety and Health Administration (OSHA). The 8-h, time-weighted average exposure limit for particles not otherwise specified is $15,000 \mu\text{g}/\text{m}^3$ for total dust with lower, sometimes much lower, values for specific compounds (OSHA 2006). The Mine Safety and Health Administration (MSHA) also has 8-h, time-weighted average exposure limits to protect miners (MSHA 2014a). These agencies specify the use of filter-based samplers to measure

aerosol mass concentrations, calculated as the mass of particles collected on the filter determined gravimetrically divided by the volume of air sampled. Although measurements made with these samplers have high accuracy and precision, gravimetric sampling and analysis is time consuming and yields no indication on the temporal variation in mass concentrations.

In some cases, these agencies allow for the use of instruments based on principles other than gravimetric measurement as long as they pass rigorous equivalency testing. For example, MSHA has mandated the use of miniaturized tapered element oscillating microbalances (TEOMs) for personal sampling in underground mines (MSHA 2006). Instruments meeting these criteria that have been deemed FEMs by the EPA include an ambient version of the TEOM and beta attenuation monitors (BAMs). These instruments provide continuous, real-time mass concentration (Macias and Husar 1976; Grover et al. 2005; Takahashi et al. 2008), but are expensive (>\$20,000) and large. OSHA has no such equivalency procedure.

Instruments based on light scattering enable real-time measurement of particle concentrations at substantially lower cost than gravimetric and equivalent methods. Integrating nephelometers, for example, measure the light scattered by an assembly of particles over a wide range of angles, and has to be correlated with mass concentration (Heintzenberg and Charlson 1996). Photometers provide a real-time indication of mass concentration inferred from the light scattered by an assembly of particles over a small angle, typically at 90 degrees from the incident light (Görner et al. 1995). Photometers, such as the personal DataRAM (pDR-1500, Thermo Scientific, Franklin, MA, USA) and DustTrakII (8532; TSI Inc., Shoreview, MN, USA), are portable photometers often used to monitor occupational exposures. Optical particle counters (OPCs) use the magnitude of light scattered to provide real-time number concentration measurements for different particle sizes (Peters et al. 2006). We refer to these devices as medium-cost with nephelometers and photometers typically ranging from \$3000 to \$10,000 and OPCs from \$7000 to \$15,000.

Recently, several manufacturers have introduced low-cost (<\$400) aerosol sensors that use light scattering to provide information on airborne particle concentration. The DC1700 (~\$400, Dylas Corporation, Riverside, CA, USA) is a commercially available laser particle counter marketed for home use in a complete, ready-to-use package (with fan to pull air through, digital readout, and data logging capabilities) that provides the number concentration of fine and coarse particles (Unger 2011). Sharp Electronics have introduced extremely low-cost sensors based on the photometric response (Sharp GP,

\$12, GP2Y1010AU0F; and Sharp DN, \$21, DN7C3CA006, Sharp Electronics, Osaka, Japan). These sensors are intended for integration into other products, such as air conditioners and air purifiers, and consequently require a microcontroller for data logging if used for air sampling.

Environmental and indoor studies have shown that the low-cost sensors correlate well with mass concentration measured by medium- and high-cost instruments (Northcross et al. 2013; Holstius et al. 2014; Steinle et al. 2015; Wang et al. 2015). Semple et al. (2013) tested the DC1700 against a photometer (AM510, SidePak, TSI Inc., Shoreview, MN, USA) for indoor exposure to quantify second-hand smoke concentrations, and reported a 0.86 coefficient of determination (R^2). In an urban setting, Holstius et al. (2014) observed that the number or mass concentration measured with the DC1700 agreed well ($R^2 = 0.99$) with that measured with an OPC (~\$12,000, GRIMM, Model 1.108, GRIMM Aerosol Technixk GmbH & Co., Ainring, Germany). Steinle et al. (2015) found that number concentration measured with the DC1700 agreed well with mass concentrations measured with a TEOM (Thermo Scientific, Franklin, MA, USA) in urban ($R^2 = 0.7$) and rural areas ($R^2 = 0.9$). For the Sharp GP sensor compared to the DustTrak DRX 8553 (TSI Inc., Shoreview, MN, USA), Budde et al. (2012) observed a mean absolute error of less than $20 \mu\text{g}/\text{m}^3$ for concentrations that ranged from $20 \mu\text{g}/\text{m}^3$ to $160 \mu\text{g}/\text{m}^3$. Wang et al. (2015) found a high correlation (R^2) of 0.98 between the Sharp GP sensor and a SidePak (TSI Inc., Shoreview, MN, USA). Literature is unavailable on the effectiveness of these sensors for use in the workplace with occupational aerosols.

Thus, the objective of the current study was to evaluate the performance of low-cost aerosol sensors (DC1700 and two Sharp sensors) for different aerosols and at high concentrations that often occur in occupational settings. First, we assessed the ability of the DC1700 to properly count and size particles into fine and coarse bins. We assessed the sensor precision and developed equations to convert sensor raw output into mass concentration. We then compared the estimated mass concentrations to those measured with high-cost instruments adjusted to gravimetric mass.

Methods and materials

Low-cost sensors

The specifications for all aerosol instruments used in this study are listed in Table 1. All medium-cost and high-cost instruments were calibrated and maintained before the experiment. All low-cost sensors were new and used

Table 1. Aerosol measurement instruments specifications used in the current work.

Device	Cost category	Cost (\$)	Size (m) (H × W × D)	Weight (g)	Sampling flow	Size range	Concentration range
DC 1700	Low	425	0.18 × 0.11 × 0.08	544	NA	>0.5 μm >2.5 μm	0–10 ⁶ #/cm ³ *
Sharp GP	Low	12	0.046 × 0.03 × 0.02	15	NA	≥0.5 μm	0.5 V/(0.1 mg/m ³)
Sharp DN	Low	21	0.05 × 0.044 × 0.02	52	NA	≥0.5 μm	1 V/(0.1 mg/m ³)
pDR-1500	Medium	<10,000	0.181 × 0.143 × 0.08	1200	1.0–3.5 L/min	1.0–10 μm	0.001–400 mg/m ³
CPC 3007	Medium		0.14 × 0.14 × 0.292	1700	0.7 L/min	10–1000 nm	1–10 ⁵ particles/cm ³
SMPS/CPC(GRIMM)	High	~60,000			1 L/min	5–1000 nm	1–10 ⁷ particles/cm ³
APS 3321	High	~20,000	0.18 × 0.3 × 0.38	10,000	5 L/min	0.5–20 μm	10,000 particles/cm ³

*Less than 10% coincidence loss at 10⁶ particles/cm³ based on the specifications provided directly from the manufacturer.

for the first time. Prior to starting the experiments in 2014, we identified low-cost sensors from six vendors (the three tested in this work and two additional sensors from Shinyei and SYhitech). We were unable to obtain reliable results from the Shinyei sensor and ultimately decided not to test the SYhitech sensor due to resource limitations.

The DC1700 displays and stores particle number concentration (in particles/0.01 ft³) in two size ranges: larger than 0.5 μm (referred to as the small bin, although this bin includes *small and large* particles); and larger than 2.5 μm (referred to as the large bin). To stay aligned with system international units, we converted DC1700 number concentrations to particles per cm³. According to the manufacturer, particle coincidence is less than 10% for concentrations less than 10⁶ particles/cm³, although the instrument provides data well above this. Concentrations greater than 231 particles/cm³ cause the internal logging register to roll over to zero, causing unreliable measurements at high concentration (Semple et al. 2013). The DC1700 is a standalone device designed by the manufacturer for in-home use that immediately works without effort or modification.

Two models of Sharp dust sensors were tested in this work: the Sharp GP and the Sharp DN. The sensing

region of both sensors is compact (0.046 m × 0.03 m × 0.0176 m) with an infrared diode that illuminates an assembly of particles, and a phototransistor positioned at 90° from the incident light that captures light scattered by the particles. As specified by the manufacturer, the sensitivity of the Sharp GP sensor (0.5 V/0.1 mg/m³) is half that of the Sharp DN sensor (1 V/0.1 mg/m³). The Sharp GP has no accommodation to move the aerosol through the device. In contrast, the Sharp DN has a virtual impactor on the inlet and a fan on the outlet of the sensing zone. Particles smaller than 2.5 μm pass through the virtual impactor with the minor flow entering the sensing zone. We programmed a microcomputer to acquire and record data every 4 s.

Detection efficiency of the DC1700

We measured the detection efficiency of the DC1700 for seven monodisperse particle sizes, using the experimental setup shown in Figure 1. A Collision-type nebulizer (Carefusion, Middleton, WI, USA) containing salt solution (NaCl 0.9 wt%, B. Braun Medical Inc., Irvine, CA, USA) was used to generate airborne droplets, which were then dried to form solid salt particles. These polydispersed salt particles were

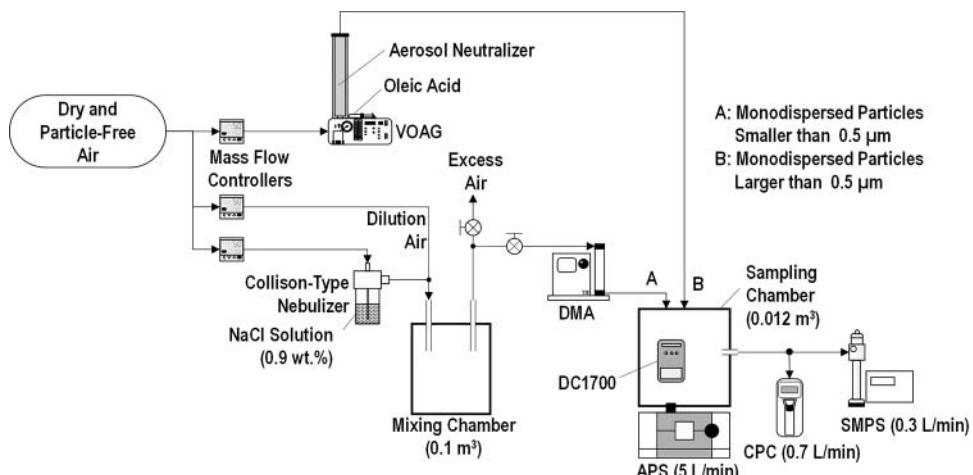


Figure 1. Experimental setup used to measure the detection efficiency of the DC1700.

passed through an electrostatic classifier (EC; 3080, TSI Inc., Shoreview, MN, USA) to produce monodispersed salt particles of 0.1 μm , 0.2 μm , and 0.3 μm size. The 0.1 μm , 0.2 μm , and 0.3 μm mobility diameters were converted to aerodynamic diameters with parameters from Table S1 (see online supplemental information (SI)). The equivalent aerodynamic diameters were 0.16 μm , 0.3 μm , and 0.4 μm , respectively. Larger monodispersed particles were produced with a vibrating orifice aerosol generator (VOAG; 3450, TSI Inc., Shoreview, MN, USA). The VOAG was operated with a 20- μm orifice, oleic acid as the solute (A195-500, Fisher Scientific, Fair Lawn, NJ, USA), and isopropanol as the solvent (A464-4, Fisher Scientific, Fair Lawn, NJ, USA). The solute-to-solution volume ratios were 1:64000 for 1.3- μm and 2- μm , 1:2370 for 3- μm , and 1:517 for 5- μm particle sizes. The liquid feed rate ranged from 2.3×10^{-5} to $4.2 \times 10^{-5} \text{ cm}^3/\text{min}$ and a frequency range of 68 to 87 kHz.

Monodispersed aerosols were passed into a sampling chamber (0.26 m \times 0.31 m \times 0.15 m). A DC1700 was positioned inside the sampling chamber with the reference instruments outside sampling directly from the chamber. The reference instruments consisted of a condensation particle counter (CPC; 3007, TSI Inc., Shoreview, MN, USA) for particles smaller than 0.3 μm and an aerodynamic particle sizer (APS; 3321, TSI Inc., Shoreview, MN, USA) for particles larger than 1.0 μm . The APS was also used to verify the sizing of particles larger than 0.5 μm . A Sequential Mobility Particle Sizer (SMPS; SMPS-C 5.402, GRIMM Aerosol Technik GmbH & Co., Ahring, Germany) with an impactor (cutoff diameter of 0.804 μm) was used to verify the monodispersed particle generation, and to ensure minimal submicrometer aerosol particle sizes were generated by the VOAG (<10 particles/cm³).

For each particle size (0.1, 0.2, 0.3, 1.3, 2, 3, and 5 μm), particle number concentration was sampled for 10 min with the DC1700 and reference instruments. We averaged the CPC and APS data to match the 1-min data from DC1700. The detection efficiency (η_D) was calculated for the fine (particles between 0.5 μm and 2.5 μm), coarse (particles larger than 2.5 μm), and total (particles larger than 0.5 μm) particles as follows:

$$\eta_D = \frac{N_{\text{DC1700}}}{N_{\text{Ref}}} \times 100, \quad (1)$$

where N_{DC1700} is the number concentration measured by DC1700 and N_{Ref} is the number concentration measured by reference instrument. A different number concentration was used for different particle sizes: fine particles

were calculated by subtracting the number concentration reported in large bin by that reported in the small bin; coarse particles were that reported in the large bin; and total particles were that reported in the small bin.

Performance of low-cost sensors

Experimental setup

The experimental setup for performance tests is shown in Figure 2a. The test chamber consisted of a mixing zone (0.64 m \times 0.64 m \times 0.66 m) and a sampling zone (0.53 m \times 0.64 m \times 0.66 m), divided by a perforated plate positioned in the middle of the test chamber. The perforated plate contained 600 evenly spaced holes, each with a diameter of 0.6 cm. The perforated plate provided a homogenous airflow with no dead zones inside the sampling zone. The aerosol from the generation systems was diluted by clean air from two HEPA filters (0.25 m³/min) and mixed with a small fan in the mixing zone. The wind speed in the sampling zone was 0.01 m/s, resulting in a Reynold number of 400 (laminar flow). Three of each low-cost sensor (DC1700, Sharp DN, and Sharp GP) and one pDR-1500 operated with an inlet cyclone (cut-off diameter of 10 μm) were positioned in the sampling zone. The pDR-1500 was operated in active mode with a 37-mm glass microfiber filter (934-AH, Whatman, USA) at the outlet. The high-cost reference instruments were outside the test chamber, with direct sampling from the sampling zone.

Five polydispersed aerosols were generated using four different aerosol generation systems as depicted in Figure 2b. Salt is a common environmental aerosol and a common test aerosol used to evaluate aerosol instruments. Arizona road dust is representative of a coarse mineral dust (Curtis et al. 2008) commonly found in environmental and occupational settings and commonly used to calibrate direct-reading instruments. Diesel fumes are common in environmental and occupational settings, and welding fume is a critical occupational hazard. To achieve two aerosols of different size with the same refractive index, salt aerosols were generated using a Collision-type nebulizer (Carefusion, Middleton, WI, USA) using two salt solutions (mass fractions of 0.9% and 5%) (Figure 2b(I)). This aerosol was diluted with clean air and mixed in a chamber (0.1 m³) to achieve desired concentrations. We used a fluidized bed aerosol generator (3400A, TSI Inc., Shoreview, MN, USA) to aerosolize Arizona road dust (Fine Grade, Part No. 1543094, Powder Technology INC., Arden Hills, MN) with the concentration adjusted by controlling the feed rate of the dust entering the fluidized bed (Figure 2b(II)). Diesel fumes were produced as exhaust from a diesel

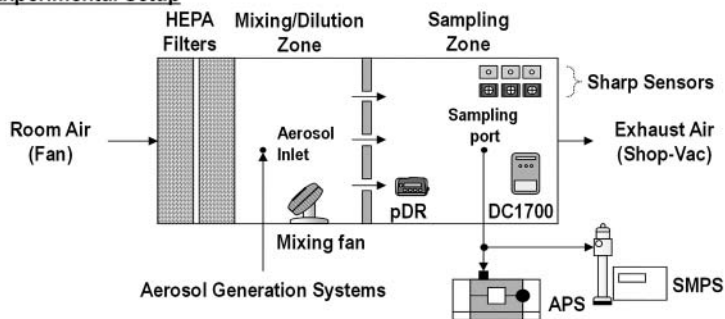
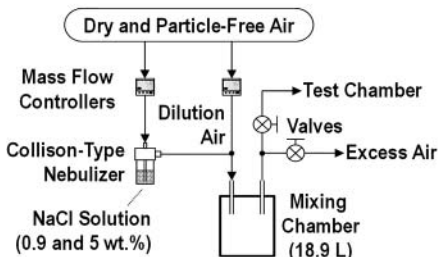
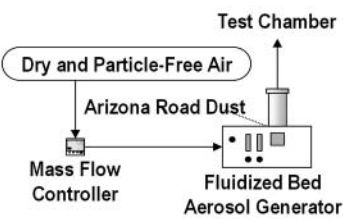
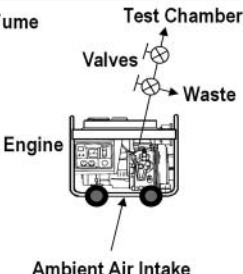
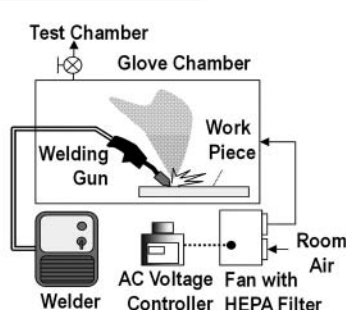
A. Experimental Setup**B. Aerosol Generation Systems****I. Salt****II. Arizona Road Dust****III. Diesel Fume****IV. Welding Fume**

Figure 2. Experimental setup used to determine the performance of low-cost sensors shown in panel (a). Schematic diagrams of aerosol generation systems shown in panel (b).

electric generator (DG6LE, Red Hawk Equipment LLC, Akron, NY, USA) with a valve used to waste fume and control concentrations (Figure 2b(III)). Welding fumes were generated with a welding system (0.03 inch Flux-Corded MIG Wire, Campbell Hausfeld, USA) operated inside a sandblast cabinet (Item 62454, Central Pneumatic, Calabasas, California, USA) (Figure 2b(IV)). To control concentrations, varying amounts of HEPA filtered air were used to push the fume from the cabinet to the sampling chamber.

The concentration of aerosols in the test chamber for each experiment fell into various ranges dependent on three factors: (1) measurable range of the DC1700 (0–231 particles/cm³); (2) maximum aerosol concentration of our experimental setup and equipment; and (3) concentration levels that range from 0 to 6500 $\mu\text{g}/\text{m}^3$. Although concentrations were lower than OSHA's occupational exposure limit for

particles not otherwise specified (15,000 $\mu\text{g}/\text{m}^3$), these concentrations are relevant to the needs of practicing industrial hygienists, who often take action to control contaminants when concentrations reach one-tenth the limit. Steady-state concentrations of test aerosols were maintained at different levels. Aerosol size distribution varied by particle type, but was approximately the same for each concentration level of the same aerosol type, except for diesel fume (Figure S2 in the online SI). For each level, the number concentration by size was measured with the SMPS three times after reaching steady-state concentration. The APS was set to record particle number concentration by size every minute throughout the experiment. Prior to starting experiments, the air in the chamber was confirmed to be clean with the pDR-1500 (0 $\mu\text{g}/\text{m}^3$) and the CPC-3007 (0 particle/cm³).

Precision and response of sensors

As a measure of sensor precision, we calculated the coefficient of variation (CV) of the raw sensor output (number concentration for DC1700 and voltage for the Sharp sensors) and after conversion to mass concentration (described below). For each minute, CV was calculated as (NIOSH 2012)

$$CV = \frac{\sigma}{\mu}, \quad (2)$$

where σ is the standard deviation and μ is the mean of the measurements from the three replicate sensors of the same type. The average of 1-min CVs obtained over all concentrations for a given aerosol were reported for each sensor. EPA's acceptable CV values for test instruments are up to 10% (EPA 2016). National Institute for Occupational Safety and Health (NIOSH) does not have a specific acceptable value for CV.

Evaluation of low-cost sensors to estimate mass concentration

We used the pDR-1500 to develop equations to convert raw output from the low-cost sensors to mass concentration. The pDR-1500 was selected as a small and portable device within the budget of many corporate industrial hygiene programs that may then potentially be used to develop correction models in the field. For each aerosol type, the mass concentrations from the single pDR-1500 were averaged to match the 1-min DC1700 measurements. These values were then adjusted by multiplying by the mass concentration measured gravimetrically with the glass microfiber filter internal to the pDR-1500 and dividing by the average of unadjusted mass concentration from pDR-1500 over the entire experiment. Different filters were used for each aerosol type measured. Linear regression was used to determine the best-fit line between the 1-min paired number concentrations of the DC1700 (small bin or total particles) and the corrected pDR-1500 mass concentrations. For the Sharp sensors, linear regression was used between the 1-min paired Sharp voltages and the corrected pDR-1500 mass concentrations.

We evaluated the mass concentrations estimated for the low-cost sensors with reference to gravimetrically adjusted mass concentration measured with the SMPS and APS following procedures specified by EPA for FEMs (40 CFR part 53, subpart C and 40 CFR part 58) and NIOSH for evaluating direct-reading gas instruments (NIOSH 2012). For each 3-min SMPS measurement, the number concentration by electrical equivalent mobility diameter from the SMPS and the number concentration by aerodynamic diameter from the APS were

converted to mass concentration by volume equivalent diameter, using the particle density and shape factor provided in Table S1 (see online SI). The reference mass concentration was calculated as SMPS/APS mass concentrations summed over all sizes multiplied by the mass concentration measured gravimetrically with the glass microfiber filter internal to the pDR-1500 and divided by the mean of unadjusted SMPS/APS mass concentrations over the entire experiment. Three-minute averages of mass concentrations from the low-cost sensors and the pDR-1500 were calculated to correspond in time with the reference concentrations. For each aerosol and sensor, Pearson coefficient (r), coefficient of determination (R^2), slope, and intercept between the sensor and reference mass concentration were determined using linear regression.

The bias (B) was calculated as (EPA 2016)

$$B = \frac{1}{n} \sum \frac{y_i - x_i}{x_i}, \quad (3)$$

where y is the estimated mass concentrations for low-cost sensor from the regression models, x is the gravimetrically filter corrected SMPS and APS mass concentrations, and n is the number of data pairs.

These parameters were compared to acceptance criteria from EPA and NIOSH. For EPA, the linear regression between measurements made with a candidate and reference instrument must have a slope of 1 ± 0.1 , a y -intercept of $0 \pm 5 \mu\text{g}/\text{m}^3$, and an $r \geq 0.97$ (40 CFR part 53, subpart C, Table C-4). EPA also specified that percent bias should be within $\pm 10\%$ (40 CFR part 58). For NIOSH, candidate and reference instruments must exhibit a slope of 1 ± 0.1 and a percent bias of $\pm 10\%$. NIOSH does not have criteria for the y -intercept (NIOSH 2012).

Results and discussion

Detection efficiency of the DC1700

The detection efficiency of the DC1700 by particle size is shown in Figure 3. Detection efficiency for fine particles was low (<2%) for submicrometer particles, increased to 52% for 1.3- μm particles, and then decreased to 29% for 5- μm particles. In contrast, detection efficiency for coarse particles consistently increased with particle size from 0% at 0.16 μm , to 10% at 1.3 μm , and 82% at 5 μm . Together, the total (fine + coarse) detection efficiency increased as particle size increased from 0.04% at 0.16 μm to greater than 100% at 5 μm .

The fact that detection efficiency was extremely low for particles smaller than 0.5 μm agrees with

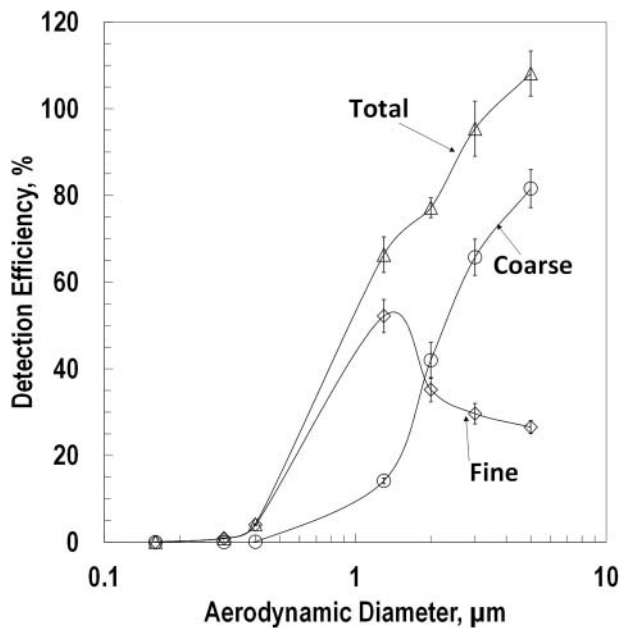


Figure 3. Detection efficiency of the DC1700 by aerodynamic diameter. Particles smaller than $0.5\text{ }\mu\text{m}$ were generated with a nebulizer followed by electrical classification, and the reference concentration was measured with the CPC. Particles larger than $1\text{ }\mu\text{m}$ were generated with the VOAG, and the reference concentration was measured with the APS. Total (fine + coarse) corresponds with the “small bin” of the DC1700 and coarse corresponds with the “large bin” of the Dylos. Fine was calculated as the small bin minus the large bin.

manufacturer specifications and is consistent with the fact that very little light is scattered by sub- $0.5\text{-}\mu\text{m}$ particles. However, it was surprising to find that the DC1700 incorrectly classified particles larger than $2.5\text{ }\mu\text{m}$ as fine particles (e.g., 29% of $5\text{-}\mu\text{m}$ particles classified as fine, Figure 3), when the detection efficiency should be zero. Similarly, the DC1700 misclassified sub- $2.5\text{-}\mu\text{m}$ into the coarse bin (e.g., 10% of $1.3\text{-}\mu\text{m}$ particles were classified as coarse). The classification of the coarse and fine bins are based on the proprietary Table in the DC1700 firmware. It is not clear why this misclassification occurred. For the remainder of the study, only the total fraction measured by the DC1700 was used, which

corresponds to the small bin. The decision was based on two factors: total detection efficiency increased with particle size; and coarse and fine particles were highly correlated ($R^2 = 0.98$).

Performance of low-cost sensors

Performance of low-cost sensors are presented for mass concentrations less than $5000\text{ }\mu\text{g}/\text{m}^3$. This decision was based on diesel fume experiments (Figure S1 in the online SI) in which the relationship between mass concentration measured with the pDR-1500 and the reference instrument was linear for concentrations $<5000\text{ }\mu\text{g}/\text{m}^3$ but nonlinear for greater concentrations. We attribute the nonlinear relationship for extremely high concentrations to particle coincidence in the sensing zone of the pDR-1500.

Precision and response of sensors

Table 2 summarizes the precision expressed as CV calculated for raw data and converted mass concentration data by sensor and aerosol type. Scatter plots of raw sensor response relative to reference mass concentrations (i.e., filter-corrected SMPS and APS data) are shown for the DC1700 in Figure 4, and for the Sharp DN and Sharp GP in Figure 5. The x-axis error bars in these figures (the standard deviation of reference measurements) indicate the variability of mass concentration at each steady state. The y-axis error bars (the standard deviation within sensor type) indicate a combination of within-sensor precision and concentration variability. We displayed Figure 5 with log–log axes to allow all data to be visible (particularly for the Sharp GP) and Figure 4 in the same way for consistency. Based on the raw measurements, the DC1700 exhibited the best precision of the three sensors with the lowest CV (2.2–14% for the small bin; and 5–15% for the large bin) and smallest error bars in the response curves (Figure 4). For the Sharp sensors, the

Table 2. Precision of low-cost sensors raw output (raw) and calculated mass concentration based on the regression model (mass) expressed as the mean coefficient of variation (CV,%) by aerosol type.

Aerosol	DC1700								
	Small bin		Large bin		Sharp DN		Sharp GP		
	Number	concentration	Mass	Raw	Mass	Voltage	Mass	Voltage	Mass
0.9% salt aerosol	2.2		1.4	7.2	—	27	5.9	14	5.9
5% salt aerosol	2.2		1.4	15	—	24	5.4	51	4.8
Arizona road dust	4.3		3.1	5.0	—	27	1.7	5.0	1.9
Diesel fume	14		1.8	12	—	17	0.8	15	0.9
Welding fume	9.0		8.0	14	—	30	7.1	2.0	1.7
Overall mean	7.4		3.1	11	—	25	4.2	17	3.1

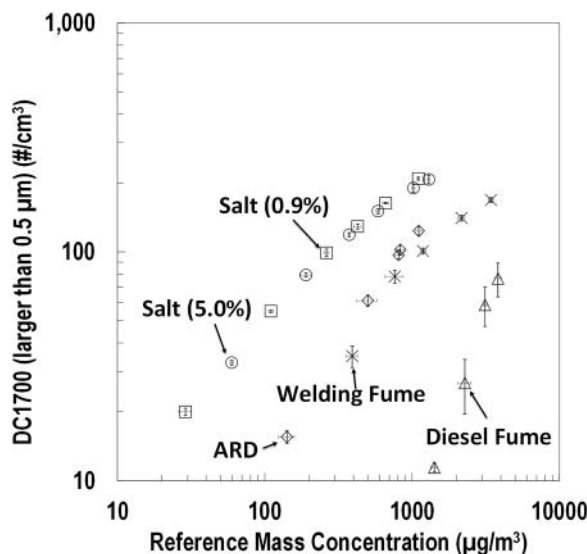


Figure 4. Raw output of the DC1700 relative to reference mass concentration for DC1700. Reference mass concentration was calculated by correcting SMPS + APS data with mass concentration measured with a gravimetric filter for each aerosol. The error bars represent one standard deviation.

CV was high for most cases, varying from 17% to 30% for the Sharp DN and from 2% to 51% for the Sharp GP.

Sensor precision is an important factor for determining an approach to estimate mass concentration from their response. The good precision of the DC1700, presumably stemming from the fact that the factory calibrates each sensor (Northcross et al. 2013), suggests that all DC1700s can be treated similarly when estimating mass concentration. In contrast, the Sharp sensors are substantially less precise, indicating the need to treat each sensor independently when computing mass concentration. In regards to the Sharp GP sensor, Budde et al. (2012) correlated multiple Sharp sensors with a Dust-Trak and reported that each sensor has different measurements. The author attributes these differences to the fact that the Sharp sensors are not factory calibrated to reproduce the same values. Wang et al. (2015) measured the precision of the Sharp GP sensor, and found that the standard deviation among devices increased with mass concentrations, concluding that the Sharp GP sensors have low precision. To our knowledge, no one has reported the precision of the DC1700.

For all sensors, aerosol type strongly influenced sensor response. The response relative to reference mass concentration for the DC1700 (Figure 4) was linear for low concentrations and deviates from linearity for particle concentrations greater than 10^6 particles/cm 3 . The change in response relative to change in mass concentration (slope) was greatest for the salt aerosol, with both salt solutions having similar slopes. The slopes for

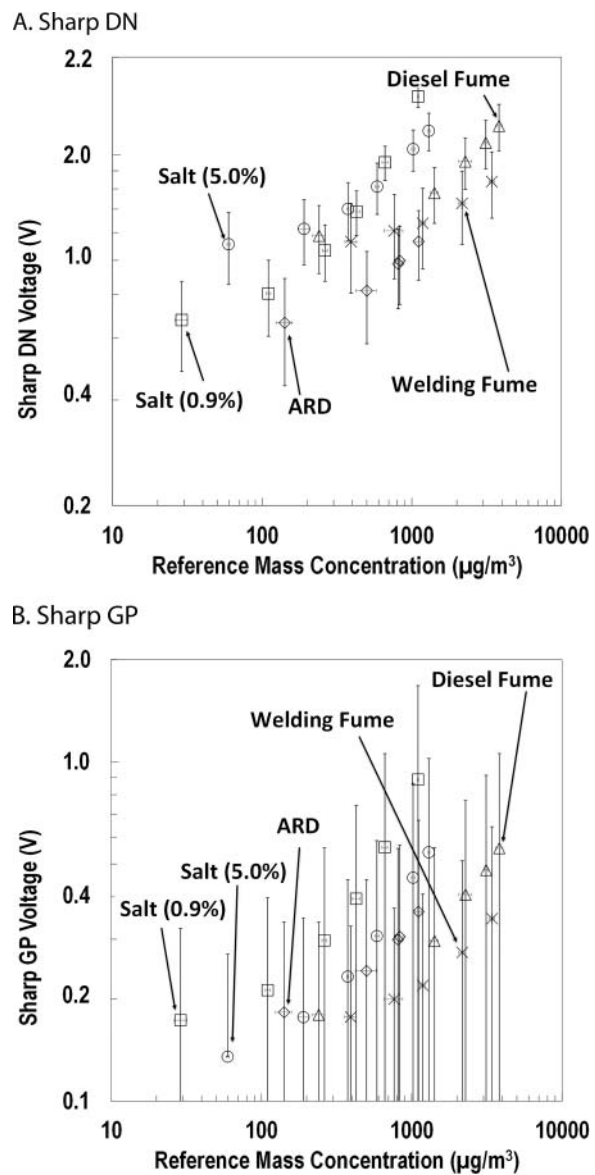


Figure 5. Raw output of the low-cost sensors relative to reference mass concentration for: (a) Sharp DN; (b) Sharp GP. Reference mass concentration was calculated by correcting SMPS + APS data with mass concentration measured with a gravimetric filter for each aerosol. The error bars represent one standard deviation.

welding fume and Arizona road dust were similar but less than that for salt aerosol. The slope was the least for the diesel fume, dramatically different from that of the other aerosols. In contrast, the response of the Sharp sensors (Figure 5) was linear for all aerosols, except for the diesel fume. The Sharp DN (Figure 5a) and Sharp GP (Figure 5b) response curves had similar correlations but with different magnitudes. The slope of the Sharp sensors was similar to that of the DC1700, except for the fact that the slope was lower for welding fume than diesel fume. The response of the Sharp GP voltage with the mass concentrations for Arizona road dust was

Table 3. The average calculated mass median diameter (MMD) and geometric standard deviation (GSD) for each aerosol based on the SMPS and APS data.

Aerosol	MMD + standard deviation (μm)	GSD + standard deviation
0.9% salt solution	0.58 ± 0.04	1.80 ± 0.04
5% salt solution	0.81 ± 0.01	1.60 ± 0.08
Arizona road dust	2.63 ± 0.09	1.00 ± 0.06
Diesel fume	Multimodal distribution, two modes* (Figure S2 in the online supplemental information, SI)	
Welding fume	Multimodal distribution, two modes* (Figure S3 in the online SI)	

*Multimodal MMD and CMD were not calculated for this work.

inconsistent with the manufacturer's published data (Sharp 2006).

The different responses for the low-cost sensors to different aerosol types is a clear indication that each sensor needs to be correlated independently with a reference instrument for different aerosol environments. Particle size distribution, refractive index, and shape affect particle light scattering. The mass median diameters (MMDs) and geometric standard deviations (GSDs) of each aerosol obtained from SMPS and APS data differed substantially (Table 3). The MMD for the 5% salt solution is higher than the 0.9% salt solution, which was expected. The MMD for the Arizona road dust was around $2.6 \mu\text{m}$. We did not calculate MMDs and GSDs for the diesel fume and welding fume aerosols because the size distributions were multimodal (see Figures S2 and S3 in the online SI, respectively). A complicating factor is that the particle size distribution of the diesel fume changed for different concentration levels (Figure S2 in the online SI). The refractive index for the salt aerosol, dust, diesel fume, and welding fumes are 1.544, 1.51, 1.465, and 1.8, respectively. Since both salt aerosols have nearly identical slopes but different MMDs, we can infer that the refractive index has a role in the response. Northcross et al. (2013) and Wang et al. (2015) both suggest that the refractive index plays a role in response variation for different aerosol types. We observed that the response of the DC1700 to diesel fumes was substantially different than that for other aerosols. This finding may relate to the fact that the refractive index of diesel fume has a high absorption component or that the size distribution shifted with particle concentration.

The finding that the response of the DC1700 for high concentrations ($>106 \text{ particles}/\text{cm}^3$) is nonlinear was expected. The nonlinear response above 106 particles/ cm^3 is consistent with coincidence as specified by the manufacturer. The performance of the DC1700 was analyzed for number concentrations below 106 particles/ cm^3 . This number concentration is equivalent to a mass concentration of $500 \mu\text{g}/\text{m}^3$ for both the 0.9% and 5%

Table 4. Regression equations to estimate mass concentration (y in $\mu\text{g}/\text{m}^3$) from DC1700 number concentration (x = small bin particles/ cm^3). For particle concentrations (x) less than 106 particles/ cm^3 .

Aerosol	Equation	R^2
0.9% salt aerosol	$y = 2.6 \times x - 22$	0.96
5% salt aerosol	$y = 6.2 \times x - 153$	0.99
Arizona road dust	$y = 8.6 \times x + 98$	0.98
Diesel fume	$y = 54 \times x + 511$	0.91
Welding fume	$y = 12 \times x - 12$	0.96

salt solutions, $1200 \mu\text{g}/\text{m}^3$ for Arizona road dust, $6300 \mu\text{g}/\text{m}^3$ for diesel fume, and $2200 \mu\text{g}/\text{m}^3$ for welding fume (Figure 4). For the Sharp GP sensor, Wang et al. (2015) found similar linear response between the low-cost sensor and the SMPS for measuring NaCl particles. For the Dylos sensor, Steinle et al. (2015), Holstius et al. (2014), Klepeis et al. (2013), and Northcross et al. (2013) all observed a linear relationship for relatively low concentrations ($<300 \mu\text{g}/\text{m}^3$), whereas Semple et al. (2013) found a nonlinear relationship for concentrations that exceeded $1000 \mu\text{g}/\text{m}^3$.

Evaluation of low-cost sensors to estimate mass concentration

Linear equations used to convert sensor raw output to gravimetrically adjusted mass concentration measured with the pDR-1500 are shown by aerosol type in Table 4. For the DC1700, we only fit data for number concentrations $<106 \text{ particles}/\text{cm}^3$ (small bin) to avoid issues with coincidence. Limiting the data to concentrations below 106 particles/ cm^3 resulted in good linear fit with an R^2 value ranging from 0.91 for welding fume to 0.99 for 5% salt solution. For the Sharp sensors, we determined a linear equation unique to each sensor and aerosol because of their low precision. These equations are not shown in this article because they cannot be used for other Sharp sensors, even for the same aerosol type.

We calculated again the CV values for the low-cost sensors based on the mass concentrations, as shown in Table 2. Based on the estimated mass concentrations, all the low-cost sensors have a low CV value that ranged from 1% to 8%. The low CV values based on the estimated mass concentrations are an indication that any sensor can be used to estimate mass concentrations once calibrated for an aerosol type.

Good agreement was observed between mass concentrations measured with the pDR-1500 and reference mass concentrations (from SMPS APS data; Table 5). Values of r were all high and the slope values were close to unity (ideal). The coefficient of determination (R^2) ranged from 0.98 to 0.99. Biases were low ranging from

Table 5. Evaluation of mass concentrations measured with the pDR-1500 with reference to those measured with the SMPS and APS.

Aerosol	Data pairs	Slope \pm std. error	Intercept \pm std. error ($\mu\text{g}/\text{m}^3$)	r	R^2	% bias
0.9% salt aerosol	21	1.2 \pm 0.02	-46 \pm 12	0.99 ¹	0.99	-3.4
5% salt aerosol	21	0.9 \pm 0.006	-5.0 \pm 4.0 ¹	0.99 ¹	0.99	4.6
Arizona road dust	18	1.3 \pm 0.04	-54 \pm 14	0.99 ¹	0.98	-2.0
Diesel fume	21	1.1 \pm 0.02 ²	28 \pm 66	0.99 ¹	0.99	-9.1
Welding fume	18	1.0 \pm 0.02	-55 \pm 24	0.99 ¹	0.99	-1.1

¹Meets EPA criterion.²Meets NIOSH criterion.**Table 6.** Evaluation of mass concentrations estimated with the DC1700 with reference to those measured with the SMPS and APS. Based on DC1700 particle concentrations less than 106 particles/cm³.

Aerosol	Data pairs	Slope \pm std. error	Intercept \pm std. error ($\mu\text{g}/\text{m}^3$)	r	R^2	% bias
0.9% salt	21	0.9 \pm 0.04	14 \pm 7.0	0.99	0.98	4.0
5% salt	21	0.8 \pm 0.05	21 \pm 7.0	0.99	0.98	7.0
Arizona road dust	18	1.2 \pm 0.04	10 \pm 26	0.98	0.98	-18
Diesel fume	21	1.1 \pm 0.05	-51 \pm 23	0.95	0.91	-38
Welding fume	18	0.9 \pm 0.07	71 \pm 67	0.98	0.95	-3.0

¹Meets EPA criterion.²Meets NIOSH criterion.

-1.1% for welding fume to -9.1% for diesel fume. These results suggest that the pDR-1500 is a good medium cost device that can be used to determine regression models for the low-cost sensors.

Table 6 summarizes the evaluation of mass concentrations estimated with the DC1700 relative to those measured with the SMPS and APS. Values of *r* and R^2 were high (an ideal value is 1). Slope values were closer to unity and biases were <10% for the salt and welding fume aerosols but exceeded 18% for the Arizona road dust and diesel fume aerosols. The DC1700 calculated mass concentrations with the reference mass concentrations are shown in Figure S4 (see online SI). The points in Figure S4 approach the one to one line. Northcross et al. (2013) also reported the linear regression between the mass concentrations estimated from the DC1700 to those from a reference instrument for three ambient sampling periods. In that work, the slope and R^2 values varied between 0.95–1.96 and 0.81–0.99, respectively.

These higher slope and lower R^2 values compared to our work may be because their study was conducted in an uncontrolled ambient setting with many different particle types sampled simultaneously.

Parts A and B of Table 7 summarize the evaluation of the Sharp DN and Sharp GP sensors, respectively. Both Sharp sensors behaved similarly. For a given aerosol, the values of slope and intercept were similar for the Sharp DN and Sharp GP sensors. For example, the Sharp DN for the 0.9% salt solution experiment measured a maximum of 2.9 volts, whereas the Sharp GP only measured 0.9 volts for the same experiment. Slopes for both sensors were near unity, ranging from 0.9 to 1.3. The coefficient of determination (R^2) ranged from 0.95 to 0.99. Biases for the sharp sensors, ranging from -9.8% to 5.2%, were substantially lower than those observed for the DC1700 (Table 6). The fact that these values were similar for both Sharp sensors can be attributed to the fact that mass concentrations were estimated from correlations with the

Table 7. Evaluation of mass concentrations estimated with the Sharp sensors with reference to those measured with the SMPS and APS.

Aerosol	Data pairs	Slope \pm std. error	Intercept \pm std. error ($\mu\text{g}/\text{m}^3$)	r	R^2	% bias
A. Sharp DN						
0.9% salt aerosol	21	1.2 \pm 0.02	-34 \pm 14	0.99 ¹	0.99	-3.7
5% salt aerosol	21	0.9 \pm 0.006	-5.0 \pm 5.0 ¹	0.99 ¹	0.99	5.2
Arizona road dust	18	1.3 \pm 0.04	-55 \pm 30	0.99 ¹	0.98	-5.8
Diesel fume	21	1.1 \pm 0.05	3.3 \pm 65 ¹	0.99 ¹	0.99	-9.8
Welding fume	18	1.0 \pm 0.02	-57 \pm 31	0.99 ¹	0.99	-1.3
B. Sharp GP						
0.9% salt aerosol	21	1.2 \pm 0.02	-33 \pm 14	0.99 ¹	0.99	-3.8
5% salt aerosol	21	0.9 \pm 0.006	-0.6 \pm 5.0 ¹	0.99 ¹	0.99	4.6
Arizona road dust	18	1.3 \pm 0.03	-56 \pm 26	0.99 ¹	0.98	-6.3
Diesel fume	21	1.1 \pm 0.025	8.2 \pm 66	0.97 ¹	0.95	-9.3
Welding fume	18	1.0 \pm 0.01	-55 \pm 25	0.99 ¹	0.99	-2.4

¹Meets EPA criterion.²Meets NIOSH criterion.

pDR-1500. The Sharp sensors calculated mass concentrations compared to the reference mass concentrations are shown in Figure S5 (see online SI). The points in Figure S5 approach the one to one line.

Bias in mass concentrations estimated with the DC1700 and reference instruments met the acceptance criterion for 0.9% salt solution, 5% salt solution, and the welding fume, but not for the other two aerosols. The correlation coefficient met EPA's criterion for all the aerosols except diesel fume. The slopes for all aerosols (excluding dust and 5% salt solution) met acceptance criterion. However, no intercepts met the acceptance criterion. For the Sharp sensors, bias and correlation coefficients met acceptance criteria. Slopes met the criterion, except for 0.9% salt and Arizona road dust aerosols. Only the intercept for 5% salt solution met the EPA criterion.

There are three main limitations to this study. The detection efficiency of the DC1700 (Figure 3) was measured using two aerosol types (salt for particles smaller than $0.3\text{ }\mu\text{m}$ and an oleic acid for particles larger than $1.3\text{ }\mu\text{m}$), which have different refractive indexes. For diesel and welding fume, assumed values for density and shape factor introduced uncertainties in reference mass concentrations from SMPS and APS data. Particles larger than 300 nm were assumed to have a constant shape factor, although Park et al. (2004) reported that shape factor increases with particle size for diesel fume and Kim et al. (2009) reported the same for welding fumes. We also assumed a constant density for diesel fume, although Park et al. (2004) reported that density decreases with particles larger than 300 nm. Lastly, the difference in MMD between salt aerosols was smaller than anticipated, yielding little information on the effect of size on sensor response.

Conclusion

We evaluated the performance of DC1700, Sharp GP, and Sharp DN low-cost sensors to measure the mass concentration of aerosols at concentrations relevant to occupational settings. The DC1700 is a stand-alone device that can be used without modification, whereas the Sharp sensors need a microcomputer for data acquisition and logging. The detection efficiency of the DC1700 was low (<5% for particles smaller than $0.3\text{ }\mu\text{m}$), increasing to 60% for $1.3\text{-}\mu\text{m}$, and to $\sim 100\%$ for particles larger than $3\text{ }\mu\text{m}$. We observed substantial misclassification of fine and coarse particles. The precision of the DC1700 sensor was high (low CVs between 2% and 15%), whereas that for the raw output of the Sharp sensors was more variable (between 2% and 51%). Although the response of the low-cost sensors was dependent on aerosol concentration, regression of sensor

output to filter-corrected mass concentrations measured with commercial mass photometer (pDR-1500) was highly effective, resulting in $R^2 > 0.97$ and reasonable bias for all sensors and aerosols. After calibration, all sensors also had high precision (<8%). This work demonstrates that once calibrated low-cost sensors can be used to measure aerosols in occupational settings at concentrations of relevance to action levels (1/10th OSHAs exposure limit for particles not otherwise specified). In future work, we will evaluate the effectiveness of using a network of low-cost sensors to assess aerosol concentrations in a field study conducted in several workplaces.

References

Antonini, J. M. (2003). Health Effects of Welding. *Crit. Rev. Toxicol.*, 33:61–103.

Budde, M., Busse, M., and Beigl, M. (2012). Investigating the Use of Commodity Dust Sensors for the Embedded Measurement of Particulate Matter. Paper presented at the Ninth International Conference on Networked Sensing Systems (INSS), Antwerp, Belgium.

Curtis, D. B., Meland, B., Aycibin, M., Arnold, N. P., Grassian, V. H., Young, M. A., and Kleiber, P. D. (2008). A Laboratory Investigation of Light Scattering from Representative Components of Mineral Dust Aerosol at a Wavelength of 550 nm. *J. Geophys. Res.*, 113:D08210. doi:10.1029/2007JD009387.

Dockery, D. W., Pope, C. A., Xu, X., Spengler, J. D., Ware, J. H., Fay, M. E., Ferris, B. G., and Speizer, F. E. (1993). An Association between Air Pollution and Mortality in Six U.S. Cities. *N. Eng. J. Med.*, 329:1753–1759.

EPA. (2006). *40 CFR Parts 53 - General Requirements for an Equivalent Method Determination (Subchapter C)*. Environmental Protection Agency, Washington, DC.

EPA. (2013). *40 CFR Parts 50, 51, 52. National Ambient Air Quality Standards for Particulate Matter; Final Rule*. Environmental Protection Agency, Washington, DC, Vol. 78, pp. 3086–3287.

EPA. (2016). *40 CFR Parts 58- Ambient Air Quality Surveillance (Subchapter C)*. Environmental Protection Agency, Washington, DC.

Görner, P., Bemer, D., and Fabriés, J. F. (1995). Photometer Measurement of Polydisperse Aerosols. *J. Aerosol Sci.*, 26:1281–1302.

Grant, W. B. (2009). Air Pollution in Relation to U.S. Cancer Mortality Rates: An Ecological Study; Likely Role of Carbonaceous Aerosols and Polycyclic Aromatic Hydrocarbons. *Anticancer Res.*, 29:3537–3545.

Grover, B. D., Kleinman, M., Eatough, N. L., Eatough, D. J., Hopke, P. K., Long, R. W., Wilson, W. E., Meyer, M. B., and Ambs, J. L. (2005). Measurement of Total PM2.5 Mass (Nonvolatile Plus Semivolatile) with the Filter Dynamic Measurement System Tapered Element Oscillating Microbalance Monitor. *J. Geophys. Res. Atmos.*, 110. doi:10.1029/2004JD004995.

Hart, J. E., Eisen, E. A., and Laden, F. (2012). Occupational Diesel Exhaust Exposure as a Risk Factor for COPD. *Curr. Opin. Pulm. Med.*, 18:151–154.

Heintzenberg, J., and Charlson, R. J. (1996). Design and Applications of the Integrating Nephelometer: A Review. *Journal of Atmos. Ocean. Technol.*, 13:987–1000.

Henneberger, P. K., and Attfield, M. D. (1997). Respiratory Symptoms and Spirometry in Experienced Coal Miners: Effects of Both Distant and Recent Coal Mine Dust Exposures. *Am. J. Ind. Med.*, 32:268–274.

Holstius, D. M., Pillarisetti, A., Smith, K. R., and Seto, E. (2014). Field Calibrations of a Low-Cost Aerosol Sensor at a Regulatory Monitoring Site in California. *Atmos. Meas. Tech. Discuss.*, 7:605–632.

Kim, S. C., Wang, J., Emery, M. S., Shin, W. G., Mulholland, G. W., and Pui, D. Y. H. (2009). Structural Property Effect of Nanoparticle Agglomerates on Particle Penetration through Fibrous Filter. *Aerosol Sci. Technol.*, 43:344–355.

Klepeis, N. E., Hughes, S. C., Edwards, R. D., Allen, T., Johnson, M., Chowdhury, Z., Smith, K. R., Boman-Davis, M., Bellettiere, J., and Hovell, M. F. (2013). Promoting Smoke-Free Homes: A Novel Behavioral Intervention Using Real-Time Audio-Visual Feedback on Airborne Particle Levels. *PloS One*, 8:e73251.

Lipsett, M., and Campleman, S. (1999). Occupational Exposure to Diesel Exhaust and Lung Cancer: A Meta-Analysis. *Am. J. Public Health.*, 89:1009–1017.

Macias, E. S., and Husar, R. B. (1976). Atmospheric Particulate Mass Measurement with Beta Attenuation Mass Monitor. *Environ. Sci. Technol.*, 10:904–907.

MSHA. (2014a). *Title 30 - Mineral Resources. Chapter I - Mine Safety and Health Administration, Department of Labor. Subchapter O - Coal Mine Safety and Health. Part 70 - Mandatory Health Standards-Underground Coal Mines. Subpart b - Dust Standards.* Mine Safety and Health Administration, Arlington, VA, Vol. 1, section 70.100.

MSHA. (2014b). Lowering Miners' Exposure to Respirable Coal Mine Dust, Including Continuous Personal Dust Monitors. *Federal Register*. Mine Safety and Health Administration, Arlington, VA, Vol. 79, No. 84, pp. 24814–24994.

NIOSH. (2012). *Components for Evaluation of Direct-Reading Monitors for Gases and Vapors.* DHHS (NIOSH) Publication No. 2012–162. National Institute for Occupational Safety and Health, Cincinnati, OH.

Northcross, A. L., Edwards, R. J., Johnson, M. A., Wang, Z.-M., Zhu, K., Allen, T., and Smith, K. R. (2013). A Low-Cost Particle Counter as a Realtime Fine-Particle Mass Monitor. *Environ. Sci. Process. Impacts.*, 15:433–439.

OSHA. (2006). Table z-1 limits for air contaminants. https://www.osha.gov/pls/oshaweb/owadisp.show_document?p_table=standards&p_id=9992.

Park, K., Kittelson, D. B., and McMurry, P. H. (2004). Structural Properties of Diesel Exhaust Particles Measured by Transmission Electron Microscopy (TEM): Relationships to Particle Mass and Mobility. *Aerosol Sci. Technol.*, 38:881–889.

Peters, T. M., Ott, D., and O'Shaughnessy, P. T. (2006). Comparison of the Grimm 1.108 and 1.109 Portable Aerosol Spectrometer to the TSI 3321 Aerodynamic Particle Sizer for Dry Particles. *Ann. Occup. Hyg.*, 50:843–850.

Seinfeld, J. H., and Pandis, S. N. (2012). *Atmospheric Chemistry and Physics: From Air Pollution to Climate Change.* John Wiley & Sons, Hoboken, NJ.

Semple, S., Apsley, A., and Maccalman, L. (2013). An Inexpensive Particle Monitor for Smoker Behaviour Modification in Homes. *Tobacco Control*, 22:295–298.

Sharp. (2006). Datasheet for Sharp Dust Sensor GP2Y1010AU0F [online]. http://www.sharpsma.com/webfm_send/1488. (accessed November 5, 2015).

Steinle, S., Reis, S., Sabel, C. E., Semple, S., Twigg, M. M., Braban, C. F., Leeson, S. R., Heal, M. R., Harrison, D., Lin, C., and Wu, H. (2015). Personal Exposure Monitoring of PM2.5 in Indoor and Outdoor Microenvironments. *Sci. Total Environ.*, 508:383–394.

Takahashi, K., Minoura, H., and Sakamoto, K. (2008). Examination of Discrepancies between Beta-Attenuation and Gravimetric Methods for the Monitoring of Particulate Matter. *Atmos. Environ.*, 42:5232–5240.

Unger, R. L. (2011). Compact, Low Cost Particle Sensor. U.S. Patent No. 8,009,290.

Wang, Y., Li, J., Jing, H., Zhang, Q., Jiang, J., and Biswas, P. (2015). Laboratory Evaluation and Calibration of Three Low-Cost Particle Sensors for Particulate Matter Measurement. *Aerosol Sci. Technol.*, 49:1063–1077.